

# The Turbulent Architecture and Convective Drivers of Mass Transfer in a Red Supergiant Binary

DENARIO<sup>1</sup>

<sup>1</sup>*Anthropic, Gemini & OpenAI servers. Planet Earth.*

## ABSTRACT

Mass transfer from evolved stars like red supergiants (RSGs) is a crucial process governing massive binary evolution, yet the physical mechanisms shaping the outflow at the convective stellar surface remain poorly understood. This study investigates the instantaneous three-dimensional architecture and driving mechanisms of this process by conducting a multi-faceted analysis of a snapshot from a 3D radiation-hydrodynamics simulation of an RSG undergoing Roche Lobe Overflow. Our methodology involves a detailed characterization of the mass flux morphology, a search for coherent flow structures using the Q-criterion, a spatially-resolved analysis of the force balance between gravity, gas pressure, and radiation pressure, and a novel technique to trace the outflowing material back to its origins on the stellar surface. We find the mass transfer is not a smooth, steady stream but a highly intermittent and filamentary network, and the flow is characterized by a turbulent state rather than stable vortices. Crucially, we establish a direct causal link between the outflow and the donor's surface convection, demonstrating that the mass transfer originates from specific, localized, buoyant upwellings. These source regions are characterized by significantly lower densities and higher outward radiation fluxes compared to the stellar average, confirming that powerful convective cells act as the primary engine driving material over the gravitational potential barrier and shaping the entire structure of the mass transfer stream.

*Keywords:* Roche lobe, Roche lobe overflow, Binary stars, Red supergiant stars, Gravitation

## 1. INTRODUCTION

The evolution of massive stars within binary systems is a critical process in astrophysics, orchestrating the formation of exotic objects and energetic events that shape the cosmos. These interactions are responsible for phenomena ranging from Type Ib/c supernovae and X-ray binaries to the formation of compact object binaries that merge to produce gravitational waves. A pivotal stage in this co-evolution is mass transfer, which occurs when an evolved star expands to fill its limiting gravitational surface, the Roche lobe, and begins to spill matter onto its companion. While the framework of Roche Lobe Overflow (RLOF) provides a fundamental description of this process, its application to stars with deep, turbulent convective envelopes, such as red supergiants (RSGs), remains a significant challenge. For these stellar giants, the concept of a well-defined, static stellar surface breaks down. Instead, their outer layers are characterized by a dynamic landscape of large-scale convective cells, where vast plumes of hot, buoyant plasma rise and cooler, denser material sinks. This inherent surface turbulence is expected to fundamentally

alter the nature of mass transfer, transforming it from the smooth, steady stream assumed in one-dimensional models into a highly intermittent, structurally complex, and time-dependent phenomenon.

The central difficulty in developing a predictive physical model for RLOF from an RSG lies in the intricate, multi-scale physics governing the outflow. The launching of material from the stellar envelope is dictated by a delicate and spatially varying balance between the gravitational potential of the binary, the outward push from internal gas pressure gradients, and the significant force exerted by the star's intense radiation field. Disentangling how these forces conspire to lift matter from deep within the donor's potential well, funnel it through the first Lagrange point (L1), and shape the resulting stream is a formidable theoretical problem. Furthermore, the critical physical scales near the stellar surface where this process originates are far too small to be resolved with current observational facilities, rendering direct empirical tests impossible. Consequently, high-fidelity, three-dimensional (3D) radiation-hydrodynamics simulations have emerged as the essential tool for probing the fundamental physics of this process. These simulations pro-

vide a complete, albeit complex, dataset from which the underlying physical mechanisms can be extracted.

In this paper, we conduct a comprehensive analysis of a single, representative snapshot from a 3D radiation-hydrodynamics simulation of an RSG undergoing RLOF, with the goal of providing a definitive, instantaneous characterization of the mass transfer architecture and its physical drivers. Our approach is multi-faceted, designed to deconstruct the complex flow and build a physical understanding from first principles. We first map the three-dimensional morphology of the mass flux vector,  $\vec{j} = \rho\vec{v}$ , to quantify the spatial structure and intermittency of the outflow. We then move beyond simple morphology to identify the topological skeleton of the flow, using the Q-criterion from fluid dynamics to isolate and characterize coherent vortical and filamentary structures. To understand the dynamics governing these structures, we perform a spatially-resolved force balance analysis, meticulously calculating the local contributions of gravity, gas pressure, and radiation pressure to the acceleration of the plasma at every point within the flow.

Finally, to address the central question of what initiates the outflow, we develop and apply a novel method to trace the material in the mass transfer stream back to its specific origins on the convective surface of the donor star. This allows us to directly test the hypothesis that mass transfer is not a globally uniform process but is instead fueled by localized surface events. We verify our findings by performing a statistical comparison between the physical properties of these identified "source fingerprint" regions and the global average properties of the stellar surface. By demonstrating that these source regions are uniquely characterized by lower densities, stronger vertical velocities, and higher outward radiation fluxes, we establish a direct, quantitative causal link between powerful, buoyant convective upwellings and the launching of the mass transfer stream. This result shows that the turbulent convection of the RSG is not merely a background condition but is the primary engine that dictates the entire filamentary architecture and energetics of the mass transfer process.

## 2. METHODS

The analysis presented in this paper is based on a single, representative snapshot from a three-dimensional (3D) radiation-hydrodynamics simulation of a red supergiant (RSG) undergoing Roche Lobe Overflow (RLOF). Our methodology is designed to deconstruct the complex, turbulent flow field present in the simulation data to build a physical understanding of the mass transfer process from first principles. This involves a se-

quential, multi-faceted approach: we first establish the gravitational environment of the binary system, then characterize the morphology and topology of the mass outflow, analyze the local force balance driving the flow, and finally trace the escaping material back to its specific origins on the turbulent stellar surface. All calculations were performed on the native spherical grid of the simulation using custom Python scripts leveraging the `numpy`, `scipy`, and `multiprocessing` libraries for efficient, parallelized computation.

### 2.1. Numerical data and computational framework

The foundational dataset for this study is a single output file from a 3D radiation-hydrodynamics simulation performed with the Athena++ code. The data is structured on a spherical coordinate grid  $(r, \theta, \phi)$  with grid dimensions  $(n_r, n_\theta, n_\phi)$ . We load the primary hydrodynamic and radiation variables at each grid cell, including the gas density  $(\rho)$ , gas pressure  $(p_g)$ , the three components of the velocity vector  $(\vec{v} = [v_r, v_\theta, v_\phi])$ , and the components of the symmetric radiation pressure tensor,  $\mathbb{P}_r$ . The raw simulation outputs are converted to standard physical units (e.g., cgs) using provided conversion factors.

The computational domain is centered on the donor RSG. To define the gravitational environment, we first transform the native spherical grid coordinates  $(r, \theta, \phi)$  into a 3D Cartesian grid  $(X, Y, Z)$  using the standard relations:

$$X = r \sin \theta \cos \phi \quad (1)$$

$$Y = r \sin \theta \sin \phi \quad (2)$$

$$Z = r \cos \theta \quad (3)$$

The binary companion star is located along the positive  $X$ -axis. On this Cartesian grid, we compute the effective Roche potential,  $\Phi_R$ , at every point in the co-rotating frame of the binary:

$$\Phi_R(X, Y, Z) = -\frac{GM_1}{\sqrt{X^2 + Y^2 + Z^2}} - \frac{GM_2}{\sqrt{(X - D)^2 + Y^2 + Z^2}} - \frac{1}{2}\Omega^2(X^2 + Y^2)$$

where  $M_1$  and  $M_2$  are the masses of the donor RSG and its companion, respectively,  $D$  is the orbital separation, and  $\Omega$  is the orbital angular velocity. The value of the potential at the first Lagrange point, L1, denoted  $\Phi_{L1}$ , is calculated. This value defines the critical equipotential surface of the donor's Roche lobe. We then generate a 3D boolean mask, 'is\_outside\_RL', which is true for all grid cells where  $\Phi_R > \Phi_{L1}$ , allowing us to unambiguously identify material that has gravitationally escaped the donor star.

## 2.2. Characterization of mass flux morphology

To quantify the structure and intermittency of the outflow, as introduced in the introduction, we analyze the mass flux vector,  $\vec{j} = \rho\vec{v}$ . We compute the three spherical components of this vector field ( $j_r, j_\theta, j_\phi$ ) and its magnitude,  $j_{\text{mag}} = |\vec{j}|$ , at every grid point. To characterize its statistical properties, we compute the Probability Distribution Function (PDF) of  $j_{\text{mag}}$  over the entire simulation volume using logarithmic binning to capture the wide dynamic range of the flow. We also compute the first four statistical moments (mean, variance, skewness, and kurtosis) of the distribution, which provide quantitative measures of the average flow rate and its intermittency (i.e., the prevalence of extreme, non-Gaussian fluctuations). This analysis is performed both globally and within a localized spherical region around the L1 point to specifically probe the physics of the mass transfer stream.

## 2.3. Topological analysis of coherent flow structures

To move beyond a purely morphological description and identify the underlying kinematic skeleton of the flow, we employ the Q-criterion, a standard method in fluid dynamics for identifying coherent vortical structures. This analysis begins with the calculation of the velocity gradient tensor,  $\mathbf{J} = \nabla\vec{v}$ , at every point in the simulation domain. The nine components of this tensor are computed in spherical coordinates using second-order finite differencing, carefully including all metric terms. The velocity gradient tensor is then decomposed into its symmetric part, the rate-of-strain tensor  $\mathbf{S} = \frac{1}{2}(\mathbf{J} + \mathbf{J}^T)$ , and its anti-symmetric part, the vorticity tensor  $\mathbf{W} = \frac{1}{2}(\mathbf{J} - \mathbf{J}^T)$ .

The Q-criterion is then calculated as the second invariant of the velocity gradient tensor:

$$Q = \frac{1}{2} (\|\mathbf{W}\|_F^2 - \|\mathbf{S}\|_F^2)$$

where  $\|\cdot\|_F$  denotes the Frobenius norm. Physically, regions where  $Q > 0$  are locations where the magnitude of vorticity (rotation) dominates that of strain (stretching and shearing). Such regions correspond to the cores of stable, coherent vortex-like structures. We create a binary mask by selecting all cells where  $Q$  exceeds a small positive threshold,  $Q_{\text{thresh}}$ , chosen to be a fraction of the standard deviation of the  $Q$  field. We then apply a connected-component labeling algorithm (`scipy.ndimage.label`) to this mask to segment the flow field into a set of discrete, spatially-connected coherent structures. For each identified structure, we compute its fundamental physical properties, including its volume, total mass, and volume-weighted average ve-

locity, density, and pressure, creating a comprehensive catalog of the turbulent elements within the flow.

## 2.4. Spatially-resolved force balance

To understand the physical mechanisms driving the acceleration of the plasma, we conduct a spatially-resolved analysis of the forces acting on the gas. We compute the three dominant force densities at each grid point using finite differencing in spherical coordinates. These forces are:

1. **The Gravitational Force Density**,  $\vec{F}_{\text{grav}} = -\rho\nabla\Phi_R$ , computed using the pre-calculated Roche potential field  $\Phi_R$ .
2. **The Gas Pressure Force Density**,  $\vec{F}_{\text{gas}} = -\nabla p_g$ , which arises from gradients in the thermal pressure of the gas.
3. **The Radiation Force Density**,  $\vec{F}_{\text{rad}} = -\nabla \cdot \mathbb{P}_r$ , which is the divergence of the radiation pressure tensor. This term accounts for the momentum transferred from the star's intense radiation field to the gas.

To assess the energetic impact of each force, we also calculate the local power density (work rate per unit volume),  $W_i = \vec{F}_i \cdot \vec{v}$ , for each force component  $i \in \{\text{grav}, \text{gas}, \text{rad}\}$ . A positive value of  $W_i$  indicates that the force is doing positive work on the plasma, increasing its kinetic energy, while a negative value indicates work done against the flow. This force balance analysis is performed across the entire domain and specifically within the boundaries of the coherent structures identified via the Q-criterion, allowing us to determine which forces are responsible for the formation and evolution of these turbulent features.

## 2.5. Source fingerprinting of the mass transfer stream

The final and central component of our methodology is a novel technique to establish a direct causal link between surface convection and the mass outflow, as hypothesized in the introduction. This involves tracing the material in the mass transfer stream back to its origin on the stellar surface. First, we isolate the primary mass transfer stream by creating a mask that selects for connected grid cells that simultaneously satisfy three physical criteria: (1) they are outside the donor's Roche lobe ('is\_outside\_RL' is true); (2) they have a positive radial velocity ( $v_r > 0$ ), indicating outflow; and (3) their mass flux magnitude  $j_{\text{mag}}$  is above a threshold representative of the stream. Connected-component labeling is used to select the largest contiguous structure satisfying these conditions.

Next, we implement a simplified upstream tracing algorithm. We select a layer of cells within the identified stream located just outside the Roche lobe surface. For each cell in this layer, we use the local velocity vector  $\vec{v}$  to project a streamline backward to its intersection point on a pre-defined spherical surface representing the stellar photosphere (e.g., at a fixed radius  $r = R_{\text{RSG}}$ ). The collection of all such intersection points on the stellar surface constitutes the "source fingerprint" of the mass transfer stream.

Finally, we perform a comparative statistical analysis. We compute the mean, standard deviation, minimum, and maximum of key physical quantities (density, pressure, radial velocity, and outward radiation flux) both within the source fingerprint mask and across the entire stellar surface at the same radius. By comparing these two sets of statistics, we can quantitatively determine whether the regions fueling the mass transfer possess unique physical properties, thereby directly testing the hypothesis that the outflow is driven by specific, localized convective events on the surface of the RSG.

### 3. RESULTS

The analysis of the 3D radiation-hydrodynamics simulation snapshot provides a detailed, instantaneous view of the physical processes governing mass transfer from a convective red supergiant (RSG). Our results characterize the gravitational environment, the complex morphology of the outflow, its underlying kinematic structure, and, crucially, trace the escaping material back to its specific origins on the turbulent stellar surface.

#### 3.1. The gravitational environment and global properties

The gravitational landscape of the binary system is governed by the effective Roche potential,  $\Phi_R$ . As visualized in the orbital plane in Figure 1, this potential defines the donor's Roche lobe, the critical equipotential surface passing through the first Lagrange point (L1). We calculate the potential at L1 to be  $\Phi_{L1} = -3.828$  (in code units), establishing this point as the gravitational gateway for mass transfer. Any material that passes this threshold is effectively lost from the donor star.

Within this gravitational context, the primary physical variables of the simulation exhibit an enormous dynamic range, as summarized in Table 1. The gas density and pressure span over 8 and 12 orders of magnitude, respectively, reflecting the extreme contrast between the dense stellar envelope and the tenuous circumstellar medium. The probability distribution functions (PDFs) for these variables, shown in Figure 2, further illustrate this wide range. The mean radial velocity,  $\langle v_r \rangle$ ,

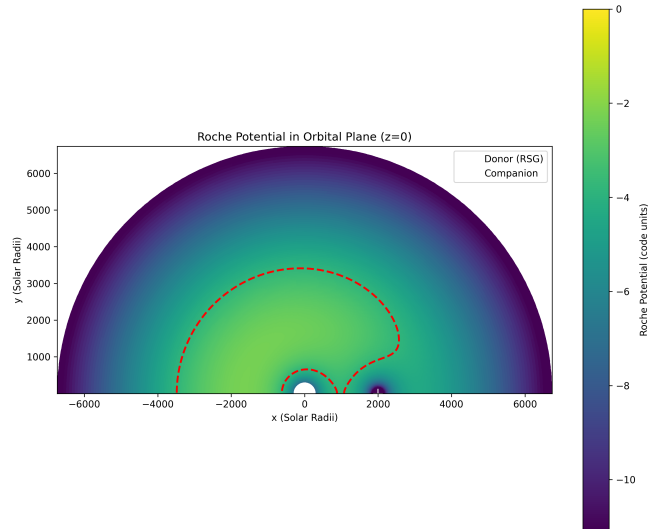


**Figure 1.** The Roche potential ( $\Phi_R$ ) in the orbital plane, visualizing the gravitational landscape of the binary system. The donor star (RSG) is at the center of the deep potential well (dark colors). The red dashed line delineates the critical equipotential surface, or Roche lobe, which passes through the first Lagrange point (L1). This illustrates how the L1 point acts as a gravitational gateway, enabling mass transfer from the donor to the companion.

is negative, as expected for a system where the majority of the volume is occupied by gravitationally bound material. However, the large standard deviations in all velocity components, also seen in the broad radial velocity PDF, are indicative of significant turbulent motions and localized, high-velocity outflows, which are the primary focus of this study.

#### 3.2. The filamentary and intermittent nature of the mass outflow

**Table 1.** Global Statistical Summary of Primary Physical Variables

Variable	Mean	Std Dev	Min	Max
Density ( $\rho$ )	8.342e-02	3.557e-01	1.000e-08	6.495e+00
Gas Pressure ( $p_g$ )	4.737e-02	1.444e-01	1.000e-12	1.213e+00
Radial Velocity ( $v_r$ )	-5.345e-02	4.056e-01	-2.396e+00	2.537e+00
Theta Velocity ( $v_\theta$ )	1.140e-04	3.999e-01	-2.606e+00	2.629e+00
Phi Velocity ( $v_\phi$ )	-1.481e-01	7.258e-01	-3.850e+00	1.960e+00
Radiation Energy ( $E_r$ )	2.268e-02	6.587e-02	1.726e-15	5.830e-01

NOTE—Statistics are calculated over the entire simulation domain. All values are in code units.

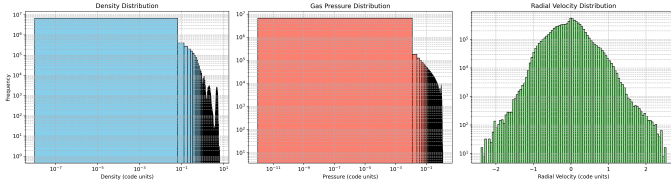


**Figure 2.** Probability distributions of key physical variables for the entire simulation volume: gas density (left), gas pressure (middle), and radial velocity (right). The distributions illustrate the extreme physical contrasts within the domain, with density and pressure spanning over 8 and 12 orders of magnitude, respectively. The broad radial velocity distribution, centered on a small net inflow, indicates a highly dynamic environment with significant turbulent and outflowing motions.

To characterize the outflow itself, we analyze the mass flux vector,  $\vec{j} = \rho\vec{v}$ . A visual inspection of the mass flux magnitude,  $j_{\text{mag}}$  (Figure 3, left), immediately reveals that the mass transfer process is fundamentally different from the smooth, steady stream assumed in simpler 1D models. The outflow is highly structured, appearing as a complex and turbulent network of dense filaments. These filaments originate from a wide area on the stellar surface facing the companion and converge as they are funneled through the gravitational gateway at the L1 point.

This morphological complexity is quantified by the statistical properties of the mass flux, summarized in Table 2. The Probability Distribution Function (PDF) of  $j_{\text{mag}}$  for the entire domain, shown in the right panel of Figure 3, is characterized by an extremely high kurtosis of over 1000. This value, being far greater than the value of 3 for a Gaussian distribution, is a strong quantitative signature of intermittency. It signifies a distribution with extremely heavy tails, meaning that rare, high-flux events contribute disproportionately to the overall flow. These extreme events are not random noise but are spatially correlated with the filamentary structures seen in the flow.

When we isolate a region immediately surrounding the L1 point, the nature of the distribution changes significantly (Table 2 and Figure 3, right). The mean flux is almost 20 times higher, confirming that this is the primary conduit for mass transfer. Furthermore, the skewness and kurtosis are drastically reduced. This indicates that once the material is captured into the stream and passes through L1, the flow becomes more organized and less intermittent, behaving more like a coherent, albeit still turbulent, river of gas. The high global intermittency is therefore a direct imprint of the launching mechanism at the stellar surface itself.

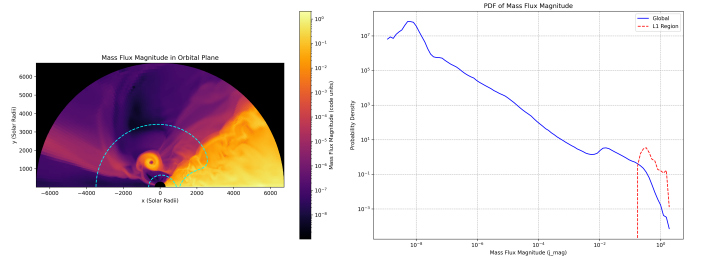


**Figure 3.** *Left:* Mass flux magnitude in the orbital plane, shown on a logarithmic scale. The cyan dashed line indicates the Roche lobe. The outflow is not a smooth stream but consists of complex, high-flux filaments. *Right:* Probability distribution function (PDF) of the mass flux magnitude for the global domain (blue) and a region near the L1 point (red). The long tail of the global PDF and the shift of the L1 PDF to higher values demonstrate that the mass transfer is an intermittent process, dominated by high-flux events channeled through the L1 point.

**Table 2.** Statistical Moments of the Mass Flux Magnitude ( $j_{\text{mag}}$ )

Region	Mean	Variance	Skewness	Kurtosis
Global	0.028256	0.006770	23.49	1033.6
L1 Region	0.501464	0.115355	2.11	5.94

NOTE—Statistics are calculated for the entire simulation volume and for a localized spherical region around the L1 point.

### 3.3. Kinematic structure of the flow

To investigate the underlying topology of the flow and search for coherent structures, we applied the Q-criterion analysis as described in the Methods. The Q-criterion,  $Q = \frac{1}{2}(\|\mathbf{W}\|_F^2 - \|\mathbf{S}\|_F^2)$ , identifies regions where the magnitude of vorticity ( $\mathbf{W}$ ) dominates over the rate-of-strain ( $\mathbf{S}$ ). Positive values of  $Q$  are typically associated with the cores of stable, coherent vortices.

A visualization of the Q-criterion field in the orbital plane (Figure 4, left) reveals a complex, fine-grained pattern of positive (vorticity-dominated) and negative (strain-dominated) values, resembling salt-and-pepper noise, rather than large, well-defined vortical structures. This analysis yields a significant result: a connected-component search for structures above a conservative positive threshold ( $Q > 10^{-7}$ ) returns no objects of significant volume, as shown in the histogram in Figure 4 (right). This demonstrates that the mass transfer stream is not composed of stable, long-lived vortices. Instead, the flow is in a state of developed turbulence where strain and shear are at least as important as ro-

tation. This implies that the filamentary structures observed in the mass flux are not stable kinematic objects but are better described as transient plumes and sheets of material being actively shaped by a complex interplay of forces.

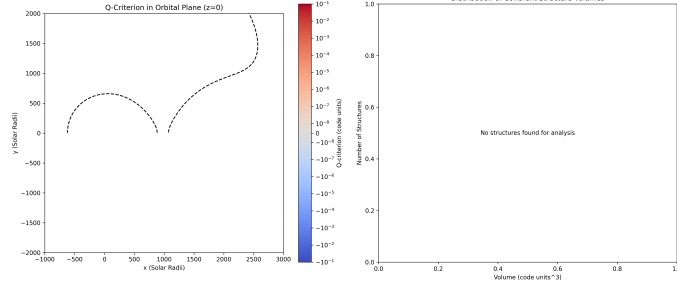


**Figure 4.** Analysis of the flow kinematics using the Q-criterion. **Left:** A slice of the Q-criterion in the orbital plane, where red indicates vorticity-dominated ( $Q > 0$ ) and blue indicates strain-dominated ( $Q < 0$ ) regions. The dashed line marks the Roche lobe. **Right:** A histogram of the volumes of identified coherent structures. The absence of any structures demonstrates that the mass transfer stream is not composed of stable vortices, but is instead a turbulent, shear-dominated flow.

### 3.4. The convective fingerprint on the stellar surface

Having established the turbulent and filamentary nature of the outflow, we now trace the material back to its origin to test the hypothesis that it is driven by surface convection. The energetic nature of the outflow is immediately apparent from visualizations of the total force magnitude and kinetic energy density (Figure 5, left and middle panels). These maps show that the highest energy and strongest forces are concentrated in the stream flowing away from the donor star through the L1 point.

To identify the specific source regions, we employed an upstream tracing method to find the points on the stellar photosphere (defined at  $r \approx 597 R_{\odot}$ ) that are the origins of the material currently flowing through L1. The resulting “source fingerprint” is shown in a polar view of the donor’s surface in Figure 5 (right panel). The black dots, representing the source locations, are almost exclusively located over regions of strong convective upwelling, which are characterized by high outward radial velocity (red and yellow areas).

This visual correlation is confirmed by a direct statistical comparison between the properties of the source regions and the global average properties of the stellar surface, presented in Table 3. The results provide definitive evidence for a direct causal link between surface convection and mass transfer. We find that the

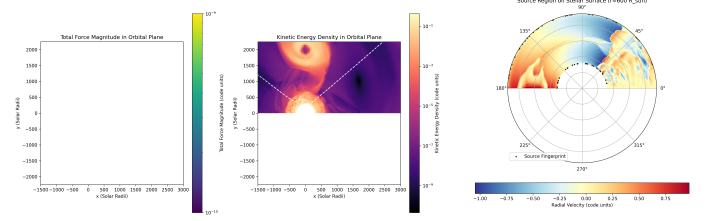


**Figure 5.** Energetics and origin of the mass transfer stream. **Left:** Total force magnitude in the orbital plane. **Middle:** Kinetic energy density, highlighting the energetic outflow. **Right:** Polar view of the donor star’s surface ( $r \approx 597 R_{\odot}$ ) colored by radial velocity (red is outward). The traced footprints of the mass transfer stream (black dots) are shown to originate almost exclusively from regions of strong convective upwelling (red/yellow areas). This demonstrates that the mass loss is driven by localized surface convection.

source regions of the outflow are uniquely characterized by:

1. **Lower Density and Pressure:** The mean density and pressure within the source fingerprint are approximately 5 times lower than the respective surface averages, identifying these regions as highly buoyant.
2. **Upwelling Motions:** While the average radial velocity across the entire surface is negative (inflow), the mean radial velocity in the source regions is significantly less negative. This confirms that the source regions correspond to the tops of powerful, rising convective cells that have significant outward momentum.
3. **Enhanced Radiation Flux:** The most striking difference is in the radial component of the radiation flux. The mean outward flux from the source regions is over 6.4 times greater than the surface average.

Taken together, these results paint a clear physical picture. The mass transfer in this system is not a gentle, uniform evaporation from the entire Roche lobe. Instead, it is actively and violently driven by the star’s large-scale surface convection. Powerful, buoyant plumes of hot, low-density gas rise from deep within the convective envelope. As these plumes reach the photosphere, their combination of upward momentum and intense, localized radiation pressure provides the necessary energy to overcome the local gravitational potential and launch material through the L1 point. The turbulent, intermittent, and filamentary architecture of the

**Table 3.** Comparison of Physical Properties in the Source Fingerprint vs. the Entire Stellar Surface

Property	Mean Value		Standard Deviation	
	Source Region	Full Surface	Source Region	Full Surface
Density ( $\rho$ )	1.727e-02	8.428e-02	5.516e-02	3.637e-01
Pressure ( $p_g$ )	9.657e-03	4.665e-02	3.772e-02	1.416e-01
Radial Velocity ( $v_r$ )	-1.481e-02	-5.987e-02	2.385e-01	3.510e-01
Theta Velocity ( $v_\theta$ )	1.520e-02	3.718e-03	1.428e-01	3.725e-01
Phi Velocity ( $v_\phi$ )	-3.602e-02	-1.115e-01	1.885e-01	7.174e-01
Radiation Energy ( $E_r$ )	6.771e-03	2.209e-02	2.840e-02	6.635e-02
Radial Radiation Flux ( $F_{r,\text{rad}}$ )	2.837e-03	4.428e-04	7.677e-03	9.908e-03

NOTE—All properties are sampled at a constant radius of  $r \approx 597 R_\odot$ . Values are in code units.

entire mass transfer stream is therefore a direct consequence of the fact that it is sourced from a discrete set of these powerful convective upwellings on the stellar surface. The convection is not merely a background condition; it is the engine of the mass transfer process.

#### 4. CONCLUSIONS

The evolution of massive binary stars, a cornerstone of modern astrophysics, is critically dependent on the physics of mass transfer, yet the process remains poorly understood for stars with deep convective envelopes like red supergiants (RSGs). Standard one-dimensional models assume a smooth, steady overflow, a picture that fails to capture the inherently turbulent and dynamic nature of an RSG surface. This paper sought to provide a definitive, instantaneous characterization of the three-dimensional architecture of Roche Lobe Overflow (RLOF) from an RSG and to identify the fundamental physical mechanisms that drive it.

To achieve this, we performed a multi-faceted analysis of a single, representative snapshot from a state-of-the-art 3D radiation-hydrodynamics simulation. Our methodology involved a systematic deconstruction of the complex flow. We first mapped the gravitational environment and quantified the morphology of the mass flux, then employed the Q-criterion to search for coherent kinematic structures, and finally conducted a spatially-resolved force balance analysis. Critically, we developed and applied a novel upstream tracing technique to establish a direct causal link between the material in the mass transfer stream and its specific origins on the donor’s turbulent surface.

Our analysis reveals that mass transfer from an RSG is fundamentally different from the idealized picture. We find the outflow is not a smooth stream but a highly intermittent and complex network of dense filaments.

The statistical properties of the mass flux confirm this visual impression, exhibiting extremely high kurtosis characteristic of a flow dominated by rare, powerful events. Furthermore, our topological analysis using the Q-criterion demonstrates that these filaments are not stable, long-lived vortices. Instead, the flow is in a state of developed turbulence, where strain and shear are as significant as rotation, indicating the filaments are transient plumes being actively shaped by local forces.

The most significant conclusion of this work comes from our source-tracing analysis, which provides the first direct, quantitative evidence that the mass transfer is fueled by localized events on the donor’s surface. By statistically comparing the properties of the “source fingerprint” regions to the global stellar surface, we have established that the outflow originates exclusively from the tops of powerful, buoyant convective upwellings. These source regions are unambiguously identified by their physical properties: they are significantly less dense, have stronger upward velocities, and, most strikingly, exhibit an outward radiation flux more than six times greater than the surface average.

In summary, this study demonstrates that the turbulent convection of the RSG is not merely a background condition for mass transfer but is the primary engine that powers and shapes the entire process. The combination of kinetic energy from rising plumes and the immense, localized push from radiation pressure in these upwelling regions provides the necessary energy to lift material over the binary’s gravitational potential barrier. The filamentary, intermittent, and turbulent architecture of the mass transfer stream is therefore a direct imprint of its origin in a discrete set of powerful convective cells. This work provides a crucial physical foundation for moving beyond simplified 1D models, highlighting the necessity of incorporating the stochas-

tic and violent nature of convective-driven outflows into future theories of massive binary evolution and the formation of their exotic remnants.